Photoplethysmogram Fits Finger Blood Pressure Waveform for non-Invasive and minimally-Intrusive Technologies
Evaluation of Derivative Approaches

Gonzalo Tapia[1], Matías Salinas[1], Jaime Plaza[1], Diego Mellado[1], Rodrigo Salas[1], Carolina Saavedra[1], Alejandro Veloz[1], Alexis Arriola[1], Juan Idiaquez[2] and Antonio Glaría[1]

[1]*Escuela de Ingeniería Civil Biomédica, U. de Valparaíso, General Cruz 222, Valparaíso, Chile*

[2]*Escuela de Medicina, U. de Valparaíso, Campus de la Salud, Angamos 655, Reñaca, Viña del Mar, Chile*

Keywords: VPG, nImI, Arterial Hypertension, Fractional Derivatives, Finapres, Photoplethysmography Derivatives.

Abstract: The purpose of this work is to fit Photoplethysmography (PPG) to finger Arterial Pressure (fiAP) waveform using derivative approaches. Derivative approaches consider using Linear Combination of Derivatives (LCD) and Fractional Derivatives (FDP$^{\alpha}$). Four informed healthy subjects, aging 35.8 ± 11.0 years old, agreed to perform Handgrip maneuvers. Signals are recorded continually; a Finapres NOVA device is used for fiAP, while a BIOPAC System is used for PPG and ECG. PPG is smoothed and segmented by heartbeat; recording sections interfered with spiky blocking noise, are eliminated. Finally, PPG is processed using LCD and FDP$^{\alpha}$ and their results are enriched using Lasso technique. Twenty records per subject at rest and twenty at raised BP are analyzed. Results show PPG to fiAP fitting errors $5.38\% \pm 0.91$ at resting fiAP and $5.86\% \pm 1.21$ at raised fiAP, being always lower than 15%, suggesting that derivative approaches could be suitable for medical applications.

1 INTRODUCTION

Invasive methods are used for Blood Pressure (BP) monitoring in critically ill patients, because measurement is more accurate introducing a cannula in the arterial system. Non-invasive procedures to measure Blood Pressure (BP) are perceived by patients as intrusive, the procedure is frequently abandoned, and the detection, monitoring and control of Arteria Hypertension (AHT) remains elusive (Kaplan, 2004). The acronym nImI stands for *non-Invasive and minimally- Intrusive* and it is proposed to summarize a concept that could be applied to medical devices (Tapia and Glaría, 2015).

In the literature, (Payne et al., 2006) established an empiric relation between Systolic Blood Pressure (SBP) and Pulse Transit Time (PTT) when an implanted BP sensor was used. (Wong et al., 2009) found new empirical relations between BP and PTT before and after subjects performed controlled running routine. (Gesche et al., 2012) has proposed a mathematical model relating the Pulse Wave Velocity and PTT according with two anthropometric parameters. (Liu et al., 2014) measured Pulse Waves with which produced PPT hysteresis. The Pulse Wave Velocity (PWV) was found in the work of (Galli et al., 2004) for vascular evaluations in patients.

In a review of Photoplethysmography (PPG) clinical applications, (Allen, 2007) alerts on artifacts that interfere its normal use, nevertheless they envisions new clinical applications supported by computational solutions (Zheng et al., 2008). (Tapia and Glaría, 2015) tried to reduce intrusiveness in detecting physical stress caused by exercise associated with rising BP, they have used an Artificial Neural Network to analyze the phase plane of two PPGs. (Baruch et al., 2011) and (Salinas, 2016) developed methodologies to decompose finger PPG components that reflect cardio-vascular characteristics. Finally, previous derivative approaches using PPG first derivative, named VPG and PPG second derivative, named APG, are reported (see (Zahedi et al., 2007) and (Elgendi, 2012)).

In this paper we propose the development of a methodology to fit PPG to the fiAP, using either a linear combination of two subsequent derivatives or using fractional derivatives (Loverro, 2004; Herrmann, 2014).

Tapia G., Salinas M., Plaza J., Mellado D., Salas R., Saavedra C., Veloz A., Arriola A., Idiaquez J. and GlarÃ■a A.
Photoplethysmogram Fits Finger Blood Pressure Waveform for non-Invasive and minimally-Intrusive Technologies - Evaluation of Derivative Approaches.
DOI: 10.5220/0006143901550162
In *Proceedings of the 10th International Joint Conference on Biomedical Engineering Systems and Technologies (BIOSTEC 2017)*, pages 155-162
ISBN: 978-989-758-212-7

2 MATERIALS AND METHODS

The required cardiovascular signal acquisition is performed in four healthy subjects (see Table 1), they were asked to answer a questionnaire, adapted from Arterial Hypertension Clinical Guide of the Chilean Ministry of Health. Twenty records per subject at rest (before Handgrip maneuver) and twenty at raised BP are analyzed (Handgrip maneuver).

Table 1: Characteristics of the subjects (S) participating in the essay. It shows their Age, Sex, Body Mass Index (BMI) and Level of Physical Activity (LPA)(Serón et al., 2010).

Subjects Characteristics				
S	**AGE**	**SEX**	**BMI**	**LPA**
1	26.2	M	18.5	Moderate
2	28.8	M	22.7	High
3	49.6	M	22.2	High
4	39.6	F	21.6	Moderate

2.1 Data Acquisition

Three non-invasive cardiovascular signals are recorded per subject at a rate of 200 Hz. For the non-deft hand, it was measured the Arterial Pressure waveform at the middle phalanx of the middle finger (fiAP) and the PPG at the tip of index finger. The electrocardiogram (ECG) is recorded in Einthoven Lead I. The fiAP signal is recorded continuously and non-invasively using the "volume-clamp" method developed by (Peňaz, 1973). This work is the base for (Finapres, 2015) and is currently implemented and improved in the Finapres new NOVA model.

Directly from fiAP, the finger Systolic (fiSYS), Diastolic (fiDIA) and Mean Arterial Pressure (fiMAP) together with Heart Rate (HR AP), and Inter-beat interval (IBI) are evaluated. After brachial oscillometric calibration, the Brachial Arterial Pressure waveform is reconstructed (reBAP) from fiAP, and brachial Systolic BP (reSYS) Diastolic BP (reDIA) and Mean BP (reMAP) are estimated from it. Oscillometric BP device Model BM 35s from Beurer is used to calibrate reSYS and reDIA. This calibration method may be inaccurate, however our proposal should also work if we use the sphygmomanometer or a cannula in a further clinical validation.

PPG and ECG are detected using a BIOPAC System configured with a MP-150 Unit and three Bionomadix Dual Biopotential Pairs. Two pairs are BN-PPGED which are connected to PPG sensors BN-PULSE-XCDR which is connected to ECG electrodes BN-EL30-Lead. PPG and ECG signals are in the bandwidths from DC to 10 Hz and from 0.3 to 35 Hz, respectively. The MP-150 unit concentrates these signal together with selected NOVA waveforms and cardiovascular trends, which are transferred to a notebook via an Ethernet cable. BIOPAC System uses proprietary signal acquisition and processing AcqKnowledge software which is installed in the notebook.

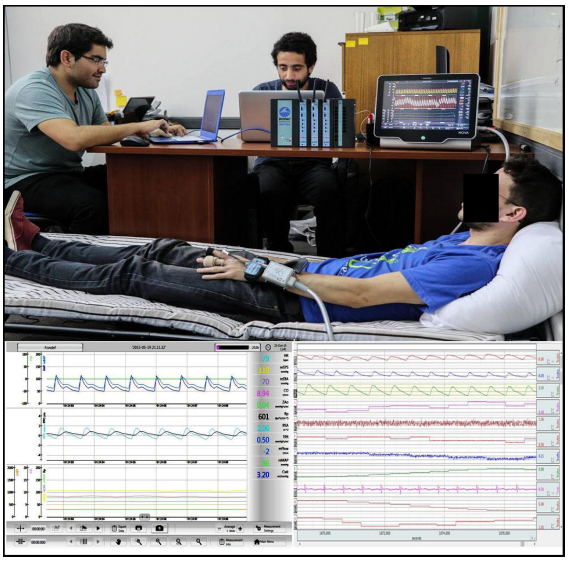

Figure 1: Data acquisition set-up.

The data acquisition set-up is shown in Figure 1. The subject of the illustrated session has, in his left hand, a PPG BN-PULSE-XCDR sensor at the tip of the index finger, and the cuff to measure fiAP from NOVA device, at the middle phalanx of the main finger. In his wrist, he has the transmitter of the Bionomadix pair. Behind the transmitter, in his forearm, he has the Finapres actuator/sensor for the cuff.

The receivers of Bionomadix pairs are at the Biopac System. The central unit of Finapres NOVA device, on one hand, sends a selected set of cardiovascular signals to Biopac MP-150 Unit; on the other hand it sends pneumatic commands to the cuff and receives the fiAP sensor signals from the Finapres actuator/sensor. Below the photograph, in the left side, it is shown the negative image of Nova device display; and in the right side, it is the display produced by the software AcqKnowledge.

A clinical essay on this work consists on a volunteer that had to lie down and stay at rest during 10 minutes after connecting all the sensors, meanwhile the NOVA is calibrated with two consecutive BP measures with the oscillometric BP device. After the complete resting time, the subject must perform two Handgrip isometric maneuvers, where he/she must press a device in a sustained manner during a standardized time (Chatterjee, 1999). The maneu-

ver is used to induce a controlled rise of the blood pressure. Both maneuvers are separated by a ten minute resting period. During the maneuver, the subject grips steadily, with his deft hand, a cuff during three minutes; the pressing is performed with one third of subjects maximal strength. Once the Handgrip is finished, the volunteer had to stay at rest during, at least, three additional minutes, and the second Handgrip, the essay is over. Essays were conducted at the School of Biomedical Engineering (EICB), Faculty of Engineering, Universidad de Valparaíso (Chile). The data set is available in Physionet Works https://physionet.org/ as a part of the project called *"Non invasive and minimally intrusive blood pressure estimates*.

2.2 PPG Signal Processing

Because PPG is sensitive to thermal changes, movements or respiration (Allen, 2007), and due to quantization errors, the raw PPG is processed with two FIR filters. Later, PPG first derivative, known as VPG, and second derivative, known as the APG, are evaluated using Five Point Stencils (FPS) algorithms. Then PPG is segmented by heartbeat. Finally and the PPG is processed to extract sections interfered with spiky blocking.

2.2.1 Pre-processing of the PPG

The derivative approaches used in this paper requires differentiating PPG once or twice. Considering that derivatives are increasingly sensitive to quantization noise as the differentiation order increases, two offline cascade preprocessing are used. First, symmetric Finite Impulse Response (FIR) filters, with Transition Bands order 19 and 399 are applied to the PPG. Low order FIR smooths the PPG by decreasing energy in quantization error frequency band. High order FIR stabilizes the DC component of the PPG.

Figure 2 illustrates the effects of smoothing the PPG and getting its baseline, differentiating the smoothed PPG using, both conventional L'Hôpital rule and Five Point Stencil (FPS) algorithm, getting VPG estimation, and differentiate the FPS processed VPG using, both conventional L'Hôpital rule and FPS algorithm, getting the APG and its baseline. The sensitivity of L'Hôpital rule to quantification error can be observed.

In the figure, the first three black signals are associated with the PPG; from top to bottom, the raw PPG, the smoothed PPG and its baseline. Next three red signals are the scaled, VPG*0.15 evaluated using both, the L'Hôpital rule, VPG*0.025, and the FPS algorithm and VPG baseline. Finally, the next three blue signals are the scaled APG*.001 using L'Hôpital rule, and FPS, APG*0.002, and its APG baseline. The illustrated signals are from a subject recorded during minute 3.07 to 3.23 of a Handgrip maneuver. PPG is FIR Low Pass filtered at 10.5 Hz and FIR High Pass Filtered at 0.25 Hz.

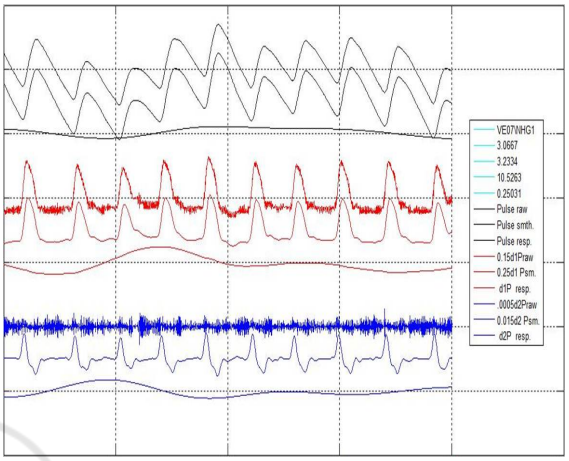

Figure 2: It is shown, from top to bottom. Black Traces: PPG raw, smoothed and PPG Baseline. Red Traces: VPG*0.15 (L'Hôpital rule), VPG*0.25 (FPS) and VPG Baseline. Blue Traces: APG*0.001 (L'Hôpital rule), APG*0.002 (FPS) and APG Baseline. Subject VE01. Recording between minutes 3.07 and 3.23. FIR: Low pass filter at 10.5 Hz; High pass filter at 0.25 Hz.

2.2.2 PPG Signal Segmentation

In order to obtain fiAP and PPG during each heartbeat, the continuous records must be segmented. A modified Pan-Tompkins (PTA) algorithm (Pan and Tompkins, 1985) is used to detect ECG R wave to segment PPG in the cardiac cycle, which is the unit of study in this work. PTA processing begins with a Band-Bass Filter, formed by a cascade of a low-pass filter (LPF), which attenuates high frequencies noises, and a High-Pass Filter (HPF), which attenuates the ECG waves P and T. The filtered signal is then derived to sharp the QRS waves with pronounced slopes. In this stage, PTA is modified, introducing Continuous Wavelet Transform (CWT) using a Mexican- Hat wavelet to detect R waves.

A threshold function is used to detect QRS complexes. For this reason the ECG is separated in 10 seconds windows to eliminate large amplitude artifacts over the whole signal. CWT is applied using a scale of 3, that is fixed during the process after an exploratory analysis finding QRS complexes. From the coefficients obtained on the 10 seconds windows, the one that have the higher amplitude is chosen to establish a searching threshold for the rest of the win-

dow. Threshold is established at the 30% of this maximum amplitude. Furthermore, a refractory time of 0.3 seconds is established (Guyton and Hall, 2011), representing the minimal period before the next QRS complex.

After R wave detection, a searching for possible missing waves is made differentiating twice the time interval from two consecutive complexes. After the detection of windows with missing R waves, a new threshold is calculated from the two QRS complexes that contain this window. The searching process is repeated until the missing R is founded, or a number of iterations is completed.

Finally, to compensate for the phase change with respect to the original ECG that the filtering process produces, a searching of a local maximum on the original signal is made to 20 ms rearwards from the positions already founded. This local maximum corresponds to the R wave on the original ECG signal.

2.2.3 Noisy PPG Extraction

While PPG is transmitted from sensor module to Biopac system, spiky communication interruption occurs and the signal is blocked. An algorithm is implemented to detect and remove the PPG segments interfered by blocking noise. The unaffected segments are isolated and saved. Furthermore, it is considered that unaffected PPG sections with less than ten segments are useless, the reasons are given below.

The local minimum of PPG wave within the 500 ms after an R wave is considered as the PPG wave beginning. To improve PPG wave discrimination from interruption artifacts, the first derivative of the segmented PPG named the VPG- is calculated using FPS algorithm. Maximum VPG is normally near the first third of cardiac cycle, while interruption artifact is not synchronized, happening at any instant within the segment.

To detect artifacts in the first third of the heartbeat, a Mexican Hat Wavelet Transform is used at scale of 15 which correlates better with artifacts than with VPG. Nevertheless, higher correlation is at artifacts minimum values, while VPG higher correlation is at its maximum values. The interruption artifacts are well detected when both parts of the algorithm are combined.

2.3 Derivative Approaches

VPG and APG have been extensively used in PPG analysis. See for example (Zahedi et al., 2007), where the effect of aging on its velocity rising edge is studied, and (Elgendi, 2012) proposes standardizing PPG terminology.

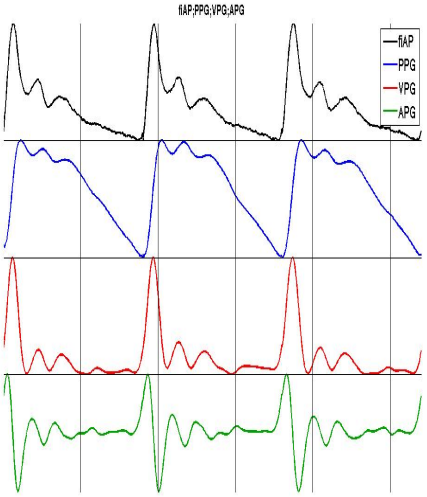

Figure 3: Temporal diagram of fiAP, PPG, VPG and APG.

During a private visit to Paul Bourgine in Paris, last February, and while talking about complex adaptive systems and large interactive networks, conversation suddenly switched towards the textbook on Fractional Calculus (Herrmann, 2014). By that time, fruitless initial efforts, trying to fit PPG with fiAP, were tested in Valparaíso. Both events triggered the idea that Fractional Derivatives (FD) would deserve a chance. During last June, Matías Salinas got surprising preliminary results, in Valparaíso, using Fractional Derivative (FD) to fit PPG to fiAP. In addition, while, trying to find an intuitive meaning of FD, Gonzalo Tapia tested with a Linear Combination of the PPG with its first Derivative (LCD). Results of fitting PPG to fiAP with LCD were again as surprising as those of Matías, although it is clearer that FD is not equivalent to LCD. The results obtained by Matías and Gonzalo are at the center of this paper.

A non explicit hypothesis, can now be formulated after these results, it could be phrased: "*the blood flow through the digital artery of the index finger can be modeled using both derivative approaches*.

Subsequently, LCD and FD are enriched using Lasso method for linear regression that combines multiple values of parameter α, either LCD and FD. The Lasso technique (Tibshirani, 1996), which consists in a penalized least squares method imposing a L_1 penalty on the regression coefficients. Let (x_i, y_i), $i = 1, 2, ..., N$ be some data, where $x_i = (x_{i1}, ..., x_{ip})^T$ are the predictor variables and y_i are the responses. As in the usual regression set-up, it is assumed either that the observations are independent or that the y_i are conditionally independent given the x_{ij}. It is assumed that the x_{ij} are standardized so that: $\sum_i \frac{x_{ij}}{N} = 0$ and

$\sum_i \frac{x_{ij}^2}{N} = 1$. Let $\hat{\beta} = (\hat{\beta_1}, ..., \hat{\beta_p})^T$, then the parameters $(\hat{\beta_0}, \hat{\beta})$ are obtained with the Lasso technique :

$$(\hat{\beta_0}, \hat{\beta}) = argmin(\sum_{i=1}^{N}(y_i - \beta_0 - \sum_j \beta_j x_{ij})^2 + \lambda \sum_j |\beta_j|)$$

where N is the number of observations, y_i is the response at observation i, x_i is data at observation i and λ is a positive regularization parameter. The parameters β_0 and β are scalar parameter. As λ increases, the number of nonzero components of β decreases.

2.3.1 Linear Combination of Derivatives

For a first approach, let $LCD^{(i)}$, be define as:

$$LCD^{(i)} = (1-\alpha)PPG^{(i)} + \alpha PPG^{(i+1)} \quad (1)$$

where $PPG^{(k)}$ is the k^{th} order temporal derivative of the PPG, and α is a single parameter to fit PPG to fiBP. Notice that, if LCD=$LCD^{(0)}$, given (1), then:

$$LCD = (1-\alpha)PPG + \alpha VPG \quad (2)$$

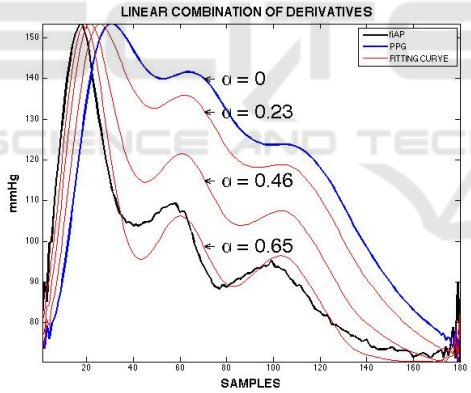

Figure 4: LCD PPG to fiAP before Handgrip maneuver.

2.3.2 Fractional Derivatives

For the second approach, Fractional Derivatives is used. The α^{th} FD of PPG (FDP^{α}) is given by:

$$FDP^{\alpha} = \frac{dPPG^{\alpha}}{dt^{\alpha}} \quad (3)$$

According to (Loverro, 2004), if $f(t) = PPG$ and $f^{\alpha}(t)=FDP^{\alpha}dt^{\alpha}$, then :

$$f^{\alpha} = \lim_{h\to 0} \frac{1}{h^n} \sum_{m=0}^{\frac{t-a}{h}} \frac{(-1)^m \Gamma(\propto +1)}{m!\Gamma(\propto -m+1)} f(x-mh) \quad (4)$$

In FD, two possible criteria are given to evaluate the derivative of a constant; Riemann-Liouville and Caputo criterium. It is decided to use the first criteria because of "physiological plausibility" (Glaría et al., 2010). In such a case, α^{th} FD of DC component of PPG, DCP^{α}, is given by

$$DCP^{\alpha} = \frac{d^{\alpha}}{dt^{\alpha}} t^0 = \frac{1}{\Gamma(1-\alpha)} t^{-\alpha} \quad (5)$$

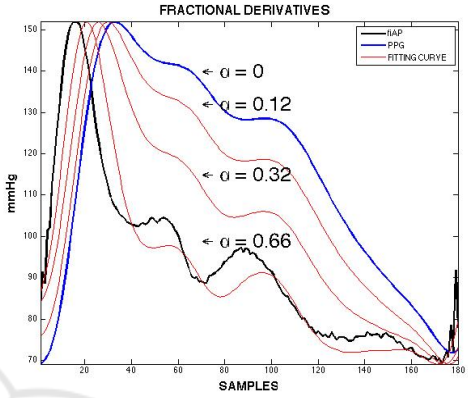

Figure 5: FD PPG to fiAP before Handgrip maneuver.

3 RESULTS

Table 2 shows the mean of fiSYS and fiDIA measured in the fiAP on each subject, at resting fiAP and at raised fiAP. There is a consistent increase in the average over the four cases, and in rest and raised fiAP; fiSYS raised, 32.5±5.9 mmHg and fiDIA raised, 26±3.1 mmHg.

Table 2: Mean fiSYS and fiDIA from fiAP before and at the end of Handgrip maneuver.

S	RESTING fiAP		RAISED fiAP	
	fiSYS	fiDIA	fiSYS	fiDIA
1	122	82	162	109
2	109	59	143	89
3	127	73	153	96
4	104	64	134	88

Table 3 is a summary for each subject comparing Root Mean Square Distance (RMSD) and the Relative Distance (R DIST) between raw PPG and fiAP.

The average over the four subjects of RMSD is 26.8±7.6 mmHg and of R DIST is 30±8.4%. On the contrary, at raised fiAP, the average of RMSD is 31.6±5.6 mmHg and the R DIST is 27.1±5.7%.

Table 4 shows the mean and standard deviation of optimal α values from the twenty resting fiAP and the

Table 3: Fitting distances: from raw PPG to fiAP waveforms before and at the end of Handgrip.

PPG EVALUATION				
S	RESTING fiAP		RAISED fiAP	
	RMSD	R DIST (%)	RMSD	R DIST (%)
1	18.6	18.8	27.3	21.1
2	34.3	37.5	36.1	39.1
3	32.3	35.6	36.9	34.2
4	22.3	28.2	26.1	24.0

Table 4: Comparison of the mean of α and its standard deviation on each subject estimated with the two methods on 20 waves before and 20 waves at the end of Handgrip.

α EVALUATION				
S	RESTING fiAP		RAISED fiAP	
	LCD	FD	LCD	FD
1	.71±.14	.74±.04	.53±.07	.67±.06
2	.72±.06	.62±.07	.74±.04	.72±.09
3	.80±.08	.84±.09	.81±.09	.90±.06
4	.71±.04	.71±.08	.72±.03	.73±.05

twenty raised fiAP, in the four subjects, using both LCD and FD. The average of α over four subjects, for both at resting fiAP, LCD is 0.74 and for FD is 0.73. In raised fiAP for LCD is 0.70 and for FD it is 0.76, suggesting that VPG clearly outweighs the PPG when fitting PPG to fiAP.

Table 5 summarize, for each subject, the Root Mean Square Error (RMSE) and the relative error (R ERR) between LCD, FD, LCD + Lasso and FD + Lasso processing with PPG. At resting fiAP, RMSE average over the four subjects, for LCD is 5.2 mmHg and R ERR is 5.4%; for FD is 6.0 mmHg and R ERR is 6.0%; for LCD + Lasso is 5.7 mmHg and R ERR is 6.1%; and, finally, for FD + Lasso is 3.9 mmHg and R ERR is 4,1%. At raised fiAP, RMSE average, over the four subjects, for LCD is 7.6 mmHg and R ERR is 6.0%; for FD is 8.3 mmHg and R ERR is 6.4%; for LCD + Lasso is 8.4 mmHg and R ERR is 6.9%; and, finally, for FD + Lasso is 5.2 mmHg and R ERR is 4,1%.

Figure 6 illustrates a comparison between the two derivative approaches, with and without Lasso, in each subject at resting fiAP.

Figure 7 shows a comparison of fitting errors relative to the initial raw PPG to fiAP distance (Blue bars), when using LCD (red bars), without and with Lasso, and FD (green bars), without and with Lasso. Errors are Evaluated using average of Relative errors plus or minus the standard deviation. It can be appreciate that the FD with Lasso outperforms with statistical significance the other models and reduce the distance between the raw PPG and fiAP from approximately 30% to 5%.

Finally, we have extended the results for a total of 15 subjects with 250 heartbeats for each subject. Due to the limit space available, we summarize the results in the total adjusting error of $5.7\% \pm 1.8$. Moreover the α is subject dependent and the value obtained was

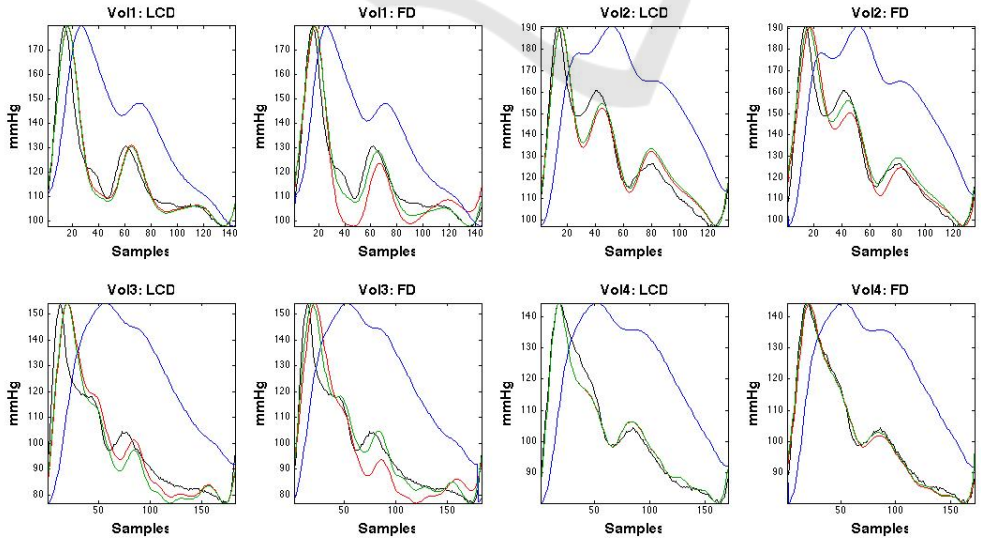

Figure 6: Four subjects, single heartbeat, before Handgrip; fitting PPG to fiAP. Top row, left to right: subject 1 fit using LCD and FD; subject 2 fit using LCD and FD. Bottom row, left to right: subject 3 fit using LCD and FD; subject 4 fit using LCD and FD. Color codes: fiAP (Black), PPG (Blue), Derivative approaches (Red), and Derivative approaches with Lasso (Green).

Table 5: Fitting errors. Top: at resting fiAP and Bottom: at Raised fiAP. From left to right: LCD fitting, FD fitting, LCD + Lasso Fitting and FD + Lasso Fitting.

FITTING ERRORS: RESTING fiAP								
	LCD		FD		LCD + Lasso		FD + Lasso	
S	RMSE	R ERR (%)	RMSE	R ERR (%)	RMSE	R ERR (%)	RMSE	R ERR (%)
1	6.3±1.4	6.8±1.7	5.2±0.5	5.4±0.5	7.5±1.7	8.2±1.9	3.5±0.5	3.7±0.6
2	3.5±0.8	3.7±0.8	5.9±1.2	5.4±1.0	3.7±1.1	4.0±1.2	3.5±0.7	3.7±0.6
3	9.1±0.8	8.5±1.2	10.1±0.7	9.9±0.9	9.5±0.9	9.3±1.2	6.7±2.2	6.5±2.0
4	1.9±0.8	2.4±1.0	2.8±0.7	3.3±0.8	2.0±0.8	2.7±1.1	2.0±0.5	2.5±0.6
FITTING ERRORS: RAISED fiAP								
	LCD		FD		LCD + Lasso		FD + Lasso	
Sub	RMSE	R ERR (%)	RMSE	R ERR (%)	RMSE	R ERR (%)	RMSE	R ERR (%)
1	10.5±4.0	8.6±3.4	9.3±1.0	7.0±0.9	12.9±5.4	11.1±4.8	5.0±0.5	3.8±0.5
2	6.2±1.1	4.6±0.7	8.1±1.1	5.7±0.9	6.4±1.2	4.8±0.8	4.9±0.7	3.6±0.5
3	9.8±2.1	7.6±1.8	10.9±1.6	8.6±1.3	10.1±2.2	8.0±2.0	7.7±1.9	6.2±1.5
4	3.7±0.5	3.1±0.4	5.0±1.5	4.4±1.3	4.2±0.7	3.7±0.6	3.1±0.8	2.9±0.8

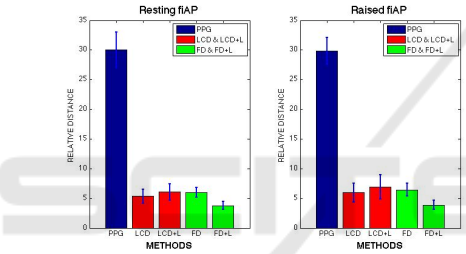

Figure 7: Relative Distances between raw PPG (Blue); LCD / LCD + Lasso (Red); and FD / FD + Lasso (Green) with the fiAP waveform.

0.73 ± 0.1.

4 CONCLUSIONS

The analysis of the results, considering that the total average fitting error is 5.7% for 15 subjects, allows to conclude that it is possible to reconstruct fiAP waveforms from the PPG using LCD and FDP$^{\alpha}$ approaches. Due to the high variability of the fitting errors per subject at resting and raised fiAP, these results suggest that the method should be customized for each subject.

Although not shown, the worst fitting error is 15%. In all cases, the fitted waveform keeps the pattern. This result suggests that derivative approaches could be suitable for medical applications. However further work must be done in order to be used for estimation purposes. On the other hand, the Fitting precision on each subject has relative low variability because it is performed in every segmented PPG wave.

When the total average of mean fitting errors, over the four subjects is ordered by performance, at rest and raised fiAP, results are, for FD + Lasso processing, 4.1 and 4.2%, for LCD processing, 5.4 and 6.0%, for FD, 6.0 and 6.4% and for LCD + Lasso, 6.1 and 6.9%. In addition, the Variation Coefficient, at rest and raised fiAP results are, for FD 15.3% and 18.3%, for LCD 25.6% and 23.4%, for LCD + Lasso, 26.7% and 24.3% and FD + Lasso 24.8% and 19.7%. Fitting PPG to fiAP at rest is always more precise (error = $5.38\% \pm 0,91$) than during raised fiAP ($5.86\% \pm 1.21$)

Finally, it should be noted that although FD algorithm requires much more complex algorithms than LCD, both approaches produce similar results. However, it is surprising that results obtained using LCD are better than those obtained with LCD + Lasso. A possible explication would be that LCD + Lasso could be penalizing twice the weights.

COMPLIANCE WITH ETHICAL REQUIREMENTS

The authors declare that they have no conflict of interest. In addition, Informed Consents were obtained and discussed with the subjects for the acquisition of fiAP, PPG and ECG from 2015 up to date. Clinical Essays have been approved by the Universidad de Valparaíso, Bioethics Institutional Committee for Human Beings Research (CIBI-SH UV for its acronym).

ACKNOWLEDGEMENTS

The authors acknowledge the support by Chilean Grants FONDEF IT13I20060 from Conicyt, CONICYT + PAI/CONCURSO NACIONAL INSERCIÓN EN LA ACADEMIA, CONVOCATORIA 2014 + Folio (79140057) and PMI UV1402 from the Ministry of Education. Thanks to anonymous subjects, either healthy volunteers or patients, who participate in Clinical Essays.

REFERENCES

Allen, J. (2007). Photoplethysmography and its application in clinical physiological measurement. *Physiological measurement*, 28(3):R1–R39.

Baruch, M. C., Warburton, D. E., Bredin, S. S., Cote, A., Gerdt, D. W., and Adkins, C. M. (2011). Pulse decomposition analysis of the digital arterial pulse during hemorrhage simulation. *Nonlinear biomedical physics*, 5(1):1.

Chatterjee, K. (1999). Physiologic and pharmacologic maneuvers in the differential diagnosis of heart murmurs and sounds. Technical report.

Elgendi, M. (2012). Standard terminologies for photoplethysmogram signals. *Current cardiology reviews*, 8(3):215–219.

Finapres (2015). Finapres medical systems (2015). http://www.finapres.com/products/finapres-nova. Accessed: 2015-04-18.

Galli, C., Camus, J. M., Fischer, E., Cabrera, I., and Risk, M. R. (2004). La velocidad de la onda del pulso en la evaluación vascular de pacientes con insuficiencia renal. *Rev Fed Arg Cardiol*, 33:212–217.

Gesche, H., Grosskurth, D., Küchler, G., and Patzak, A. (2012). Continuous blood pressure measurement by using the pulse transit time: comparison to a cuff-based method. *European journal of applied physiology*, 112(1):309–315.

Glaría, A., Taramasco, C., and J., D. (2010). Methodological proposal to estimate a tailored to the problem specificity mathematical transformation: Use of computer intelligence to optimize algorithm complexity and application to auditory brainstem responses modeling. In *Advanced Information Networking and Applications Workshops (WAINA), 2010 IEEE 24th International Conference on*, pages 775–781.

Guyton, A. C. and Hall, J. E. (2011). *Tratado de fisiología médica*. Elsevier,, Barcelona, 12 edition.

Herrmann, R. (2014). *Fractional calculus: An introduction for physicists*. World Scientific, Singapore.

Kaplan, N. (2004). *Hipertensión arterial sistémica: mecanismos y diagnóstico, in Braunwald (Ed) Tratado de cardiología*. Madrid: Marban Libros.Edition 6.

Liu, Q., Yan, B. P., Yu, C.-M., Zhang, Y.-T., and Poon, C. C. (2014). Attenuation of systolic blood pressure and pulse transit time hysteresis during exercise and recovery in cardiovascular patients. *IEEE Transactions on Biomedical Engineering*, 61(2):346–352.

Loverro, A. (2004). Fractional calculus: history, definitions and applications for the engineer. *Rapport technique, University of Notre Dame: Department of Aerospace and Mechanical Engineering*.

Pan, J. and Tompkins, W. J. (1985). A real-time QRS detection algorithm. *IEEE transactions on biomedical engineering*, (3):230–236.

Payne, R., Symeonides, C., Webb, D., and Maxwell, S. (2006). Pulse transit time measured from the ecg: an unreliable marker of beat-to-beat blood pressure. *Journal of Applied Physiology*, 100(1):136–141.

Peňaz, J. (1973). Photoelectric measurement of blood pressure, volume and flow in the finger. In *Digest of 10th International Conference on Medical Biological Engineering, Dresden, East Germany*, page 104.

Salinas, M. (2016). Hacia una tps wk para la estimación de la presión arterial. Unpublished Degree Work to obtain the Title of Ingeniero Civil Biomédico. U. de Valparaíso, Chile.

Serón, P., Muñoz, S., and Lanas, F. (2010). Nivel de actividad física medida a través del cuestionario internacional de actividad física en población chilena. *Revista médica de Chile*, 138(10):1232–1239.

Tapia, G. and Glaría, A. (2015). Artificial neural network detects physical stress from arterial pulse wave. *Revista Ingeniería Biomédica*, 9(17):21–34.

Tibshirani, R. (1996). Regression shrinkage and selection via the lasso. *Journal of the Royal Statistical Society. Series B (Methodological)*, pages 267–288.

Wong, M. Y.-M., Poon, C. C.-Y., and Zhang, Y.-T. (2009). An evaluation of the cuffless blood pressure estimation based on pulse transit time technique: a half year study on normotensive subjects. *Cardiovascular Engineering*, 9(1):32–38.

Zahedi, E., Chellappan, K., Ali, M. A. M., and Singh, H. (2007). Analysis of the effect of ageing on rising edge characteristics of the photoplethysmogram using a modified windkessel model. *Cardiovascular Engineering*, 7(4):172–181.

Zheng, D., Allen, J., and Murray, A. (2008). Determination of aortic valve opening time and left ventricular peak filling rate from the peripheral pulse amplitude in patients with ectopic beats. *Physiological measurement*, 29(12):1411.